MAGNETIC RESONANCE IN MEDICINE **19**, 221–227 (1991)

Intravoxel Incoherent Motion Imaging Using Spin Echoes*

DENIS LE BIHAN† AND ROBERT TURNER‡

†*Diagnostic Radiology Department, The Warren G. Magnuson Clinical Center and* ‡*Biomedical Engineering and Instrumentation Program, National Institutes of Health, Bethesda, Maryland 20892*

Received February 1, 1991; revised February 26, 1991

The purpose of this paper is to review the basic principles of diffusion measurement with spin echoes. These principles can be combined with those of MR imaging to generate maps of diffusion coefficients. Diffusion imaging can be extended to imaging of other intravoxel incoherent motions (IVIM), such as blood microcirculation. Some of the technical problems encountered when implementing IVIM imaging are presented. © 1991 Academic Press, Inc.

The effects of diffusion on the NMR spin-echo signal have been described long ago and used extensively in physics and chemistry. The recent coupling of diffusion NMR techniques with *in vivo* NMR imaging represents a challenging and somewhat unpredicted development. Measuring molecular displacements of water in biological tissues *in vivo* may have enormous impact, from the determination of cell exchanges to the emergency management of stroke patients, or the monitoring of laser surgery (*1*). A variety of imaging schemes has been proposed for diffusion imaging. The spin-echo method (*2–4*) is certainly the simplest to implement and has the advantage of serving as an academic example.

EFFECT OF DIFFUSION ON MR SPIN ECHOES

In the presence of a magnetic field gradient, random spin displacements produce random phase shifts which destructively interfere with each other, resulting in incomplete refocusing of the echo, and thus in an attenuation of the echo amplitude. Due to the Gaussian shape of the probability distribution of diffusion displacements, this attenuation A has an exponential dependence:

$$A = \exp(-b \cdot D). \qquad [1]$$

D is the diffusion coefficient and b a factor that depends only on the magnetic field gradients. For a constant gradient G applied during the echo delay TE of a spin-echo sequence (Fig. 1), one has (*5*)

$$b = \gamma^2 G^2 \mathrm{TE}^3/12, \qquad [2]$$

so that the echo signal S is

* Presented at SMRM Workshop of Future Directions in MRI of Diffusion and Microcirculation, Bethesda, MD, June 7 and 8, 1990.

0740-3194/91 $3.00

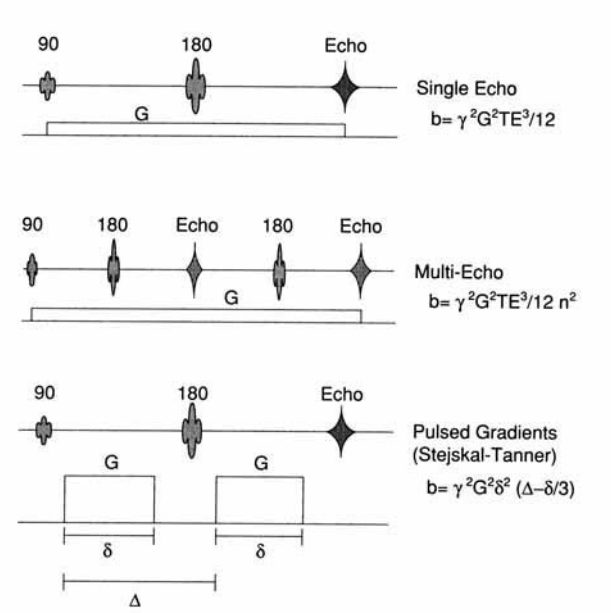

FIG. 1. Gradient factor b for different sequence designs. The spin-echo signal attenuation due to diffusion depends largely on the gradient pulse scheme used. The largest effect is produced by a constant gradient pulse in a single echo sequence.

$$S = S_0(N, \mathrm{T1}) \cdot \exp(-\mathrm{TE}/\mathrm{T2}) \cdot \exp(-\gamma^2 G^2 \mathrm{TE}^3 D/12), \quad [3]$$

where N refers to spin density and γ is the gyromagnetic ratio.

In the case of a multiple echo train, due to the refocusing at each echo, the diffusion measurement time is split in a series of shorter diffusion times equal to the interecho delay and the effect of diffusion is decreased. The b factor becomes (*6*)

$$b = \gamma^2 G^2 \mathrm{TE}^3/12\, n^2, \quad [4]$$

where n is the echo number and TE the effective echo delay of the nth echo. It follows that a single echo is more sensitive to diffusion than a multiple echo sequence.

Diffusion measurements using spin echoes have been greatly improved, in particular by using very large, but short, gradient pulses disposed on each side of the 180° pulse of a spin-echo sequence (Fig. 1) and balanced for "static" spins. In this "Stejskal–Tanner" sequence (*7*), the expression for b becomes

$$b = \gamma^2 G^2 \delta^2 (\Delta - \delta/3), \quad [5]$$

where δ is the duration of each gradient pulse and Δ the time interval separating their onset (Fig. 1). An interesting feature of this sequence is that the diffusion measurement time, equal to $(\Delta - \delta/3)$, is exactly known and controllable independently of TE. This is particularly useful for restricted diffusion studies where the diffusion time must be varied (*8*). On the other hand, it is desirable to avoid the presence of a gradient of large amplitude during the recording of the echo signal. Such a gradient would increase the frequency bandwidth and reduce the signal-to-noise ratio. With the Stejskal–

Tanner sequence, the gradient pulses which are necessary for imaging will be physically independent from the gradient pulses used for diffusion sensitization.

PRINCIPLES OF DIFFUSION IMAGING USING SPIN ECHOES

For a typical 2DFT spin-echo imaging sequence which contains multiple low amplitude gradient pulses, the effect of diffusion is completely negligible (*3*). One may thus increase diffusion sensitivity by incorporating additional gradient pulses within the imaging sequence (Fig. 2). The images therefore become "diffusion-weighted." For quantification purposes, it is necessary to determine the degree of diffusion-weighting by calculating the gradient factor b. Due to the multiple pulses used in an imaging sequence, the expression for b becomes more complicated. A general expression, which can be solved either analytically or numerically, is

$$b = \gamma^2 \int_0^{TE} |\mathbf{k}(t)|^2 \cdot dt \qquad \text{with} \qquad \mathbf{k}(t) = \int_0^t \mathbf{G}(t') \cdot dt', \qquad [6]$$

where $\mathbf{G}(t')$ is replaced by $-\mathbf{G}(t')$ for $t' > TE/2$.

If diffusion is anisotropic, one must handle separately the different components of the diffusion tensor:

$$A = \exp(-\sum_{i=x,y,z} b_i \cdot D_{ii}). \qquad [7]$$

Knowing the "b factor" associated with each image, it is possible to compute diffusion images, i.e., maps where the diffusion coefficient is displayed in each pixel, by at least two of such images differently sensitized to diffusion, but identical with respect to other parameters, such as T1 or T2. For instance, in the case of two images $S_1(x, y, z)$ and $S_0(x, y, z)$ obtained with gradient factors, b_1 and b_0, the diffusion coefficient can be determined in each pixel from the relative signal intensities according to (*2, 3*):

$$D(x, y, z) = \ln[S_0(x, y, z)/S_1(x, y, z)]/[b_1 - b_0]. \qquad [8]$$

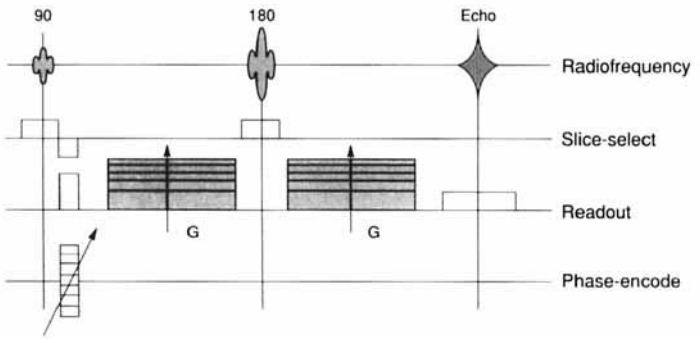

FIG. 2. Diffusion imaging sequence. Sensitization of a spin-echo 2D FT imaging sequence to diffusion can be easily obtained by inserting additional gradient pulses of variable amplitude within the sequence. These pulses (dashed boxes) can be set on any axis.

Diffusion coefficients can be evaluated more accurately from multiple images obtained with different b values using a linear regression algorithm, or, better, nonlinear iterative fitting algorithms.

Using the spin-echo scheme, it is possible to vary the direction of the diffusion-sensitizing gradients in order to enhance anisotropic diffusion effects (*9*) or their strength or duration (*10, 11*). When performing a diffusion coefficient measurement, one should, however, be careful that the diffusion time remains constant for all the images used to calculate this coefficient, if we expect diffusion to be restricted. Physically, restricted diffusion means that molecules are confined within a limited diffusion space by boundaries, so that the diffusion distance, reflected in the measured diffusion coefficient, depends on the diffusion time made available to molecules to diffuse (*8*). The only correct approach, in this situation, is to change only the gradient amplitude and to repeat, eventually, each set of measurements using different diffusion times.

It must also be pointed out that mixing "imaging" and "diffusion" gradient pulses may result in cross-terms that may not be negligible; even the imaging gradient pulses have a low amplitude (Fig. 3). These cross-terms make the Stejskal–Tanner equation (Eq. [5]) most often inadequate, resulting in overestimated values of the diffusion coefficients (*12*), and the use of an exact analytical or numerical solution of Eq. [6] must always be preferred.

Intravoxel Incoherent Motion (IVIM) Imaging—Blood Microcirculation

Since any distributed spin movement within a voxel will be responsible for spin-echo signal attenuation, the concept of diffusion imaging must be extended to all other

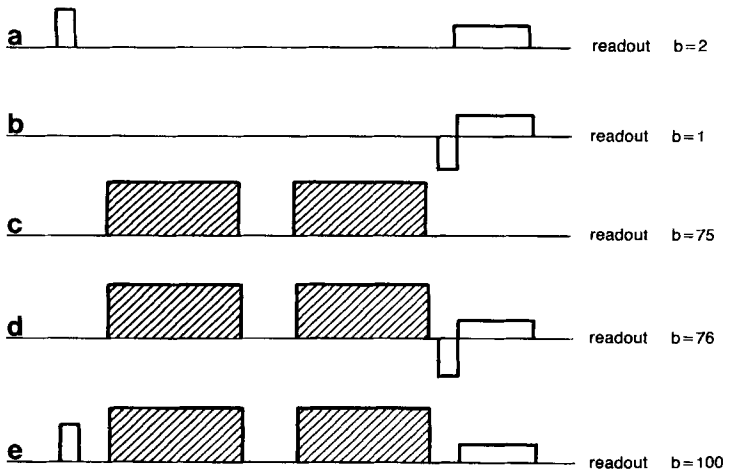

FIG. 3. Effect of cross-terms. The gradient b factor produced by conventional imaging gradient pulses is usually negligible, depending on pulse strength (field of view), duration, and intervals (a and b). The "diffusion" gradients deliberately produce larger b values to enhance the diffusion effect (c). These gradients combine their effect with the imaging gradients in a multiplicative manner (cross-terms); therefore these cross-terms may have a significant contribution to the b factor (e). The contribution of the imaging and the diffusion gradients is additive only if these pulses are not interleaved; i.e., refocusing for static spins occurs between each gradient pulse pair (d).

types of intravoxel incoherent motion. In the presence of such motion, this additional signal attenuation leads to overestimation of diffusion coefficients. This is why it has been suggested to replace the term diffusion imaging by IVIM imaging and to refer the results of the measurements to as "*a*pparent *d*iffusion *c*oefficients" (ADC) (*3, 13*).

An example of intravoxel incoherent motion is certainly blood microcirculation in randomly oriented capillary segments. Given the tortuosity of the capillary network in most tissues, such as brain, it is legitimate to consider microcirculation as pseudo-diffusive at the voxel scale. The pseudo-diffusion coefficient, D^*, associated with it depends on capillary geometry and blood velocity and is estimated to be about 10 times larger than the diffusion coefficient of water (*13*). The microcirculation contribution to the signal attenuation, A_p, is thus

$$A_p = f\exp(-bD^*), \qquad [9]$$

where f is the fractional voxel volume occupied by flowing blood (in ml of blood/100 mg of tissue water, assuming tissue density is unity). The knowledge of f and D^* would fully characterize tissue perfusion (in terms of ml/100 mg/min), for a particular capillary geometry (*14*). The difference of about an order of magnitude between D and D^* should allow microcirculation and diffusion to be separately determined. Assuming a very simple bicompartment model, i.e., "static" tissue versus flowing blood, both having similar T1 and T2, the signal attenuation becomes biexponential (*13*):

$$S = S_0(N, \mathrm{T1})\cdot\exp(-\mathrm{TE}/\mathrm{T2})\cdot\{(1-f)\exp(-bD) + f\exp[-b(D+D^*)]\}. \qquad [10]$$

For large b values, the microcirculation contribution vanishes and we are left with tissue diffusion. For small b values, both diffusion and microcirculation effects are present (Fig. 4). An ADC image calculated from two images will thus be more or less contaminated with microcirculation, depending on the b value used, justifying the concepts of IVIM imaging and ADC measurements.

Indeed, useful information on perfusion must be derived from D^* and f, as obtained when fitting data with Eq. [10], using a nonlinear iterative algorithm. Their accurate determination requires, unfortunately, since f is usually very small, many acquisitions with different b values and high signal:noise ratios, incompatible with clinical requirements due to lengthy acquisition times when conventional 2D FT imaging techniques are used. Single-shot techniques, such as EPI (*15, 16*), have dramatically improved this situation.

Implementation of Diffusion Imaging

Diffusion imaging makes high demands on imaging hardware stability (both rf and gradient systems), and the large magnetic field gradients which are required can cause eddy currents in surrounding structures with severe consequences for image analysis. Eddy currents generated in the conductive parts of the unit produce themselves magnetic field gradients which interfere with the sequence gradient pulses, and may result in image distortion or inhomogeneities across the image. As diffusion images are calculated from images which are differently sensitized to diffusion by different gradient

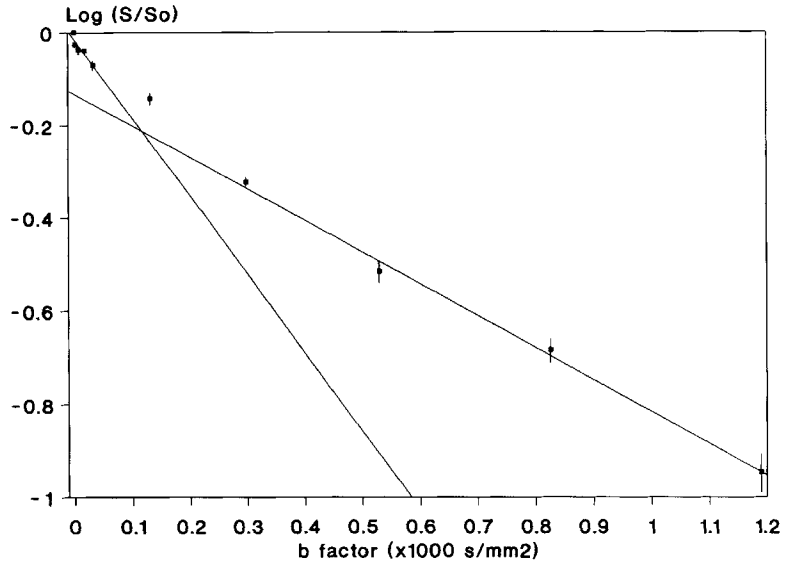

FIG. 4. Signal attenuation curve in cat brain cortex. Plot of the logarithm of the signal attenuation versus the gradient factor b. Pure diffusion effects are found in the straight part of the attenuation curve seen for large b values ($D = 0.72 \pm 0.01\ 10^{-3}$ mm^2/s). The deviation from this straight line observable for small b values has been ascribed to intravoxel incoherent microcirculation effects. The intercept gives an estimation of the perfusion factor ($f = 8.3\% \pm 0.6\%$). The slope of this initial part of the curve gives the pseudo-diffusion coefficient D^* ($6.5 \pm 0.9\ 10^{-3}$ mm^2/s). (Studies performed on a 4.7 T CSI system)

pulses, eddy current effects will appear with different magnitudes and may severely impair the measurements. To overcome eddy current artifacts, one can manage "safe" intervals between each gradient pulse, if the eddy current time constants are not too long. One may also increase the ramp time of each pulse to limit the intensities of eddy currents. Both attitudes will result in incompressible echo times that may be too long. The best solution is thus to use a set of actively shielded gradients with which eddy currents are significantly decreased.

Another major problem occurring with *in vivo* imaging of diffusion arises from irregular motion of the object. The sequences used are deliberately sensitized to motion by the addition of large gradients, and hence bulk motions may lead to widely dispersed and potentially misleading artifacts. These artifacts arise from discontinuities that occur between the successive cycles of a 2D FT sequence, which are separated by a time interval TR which is close to the motion period. Results of such temporal incoherence are commonly visible as "ghosts" along the phase-encode direction. These ghosts are particularly intense in the presence of the diffusion gradients and make the diffusion measurements meaningless. Patients must be comfortably secured within the magnet. However, the main problem comes from internal motion that occurs with respiratory and cardiac motion. Diffusion imaging in extremities and brain is the easiest, but some precautions are required before assessing measurements, because tissues may be pulsing in synchronism with pulsations in large blood vessels. Cardiac gating has been used to mitigate this problem (*13*), but even this motion is not strictly

cyclic, and random involuntary motion cannot be dealt with by this means (*17*). Motion-compensated sequences could also be used. Each of the diffusion-probing gradient pulses is bipolar in order to cancel dephasings produced by moving spins (*18*). Unfortunately, this gradient design greatly reduces the diffusion effect, so that much larger gradient amplitudes are necessary. Furthermore, motion compensation occurs only for spins moving with a constant velocity. Ultimately, the only way to avoid motion artifact is to use a single-shot technique, such as EPI (*15, 16*).

ACKNOWLEDGMENTS

The authors thank Drs. Chrit Moonen, Peter Van Zijl, James Pekar, and Mr. Daryl Despres, from the *In Vivo* NMR Research Center, National Institutes of Health, for helpful discussions and for help in acquisition of the data presented in Fig. 4.

REFERENCES

1. D. LE BIHAN, *JMRI* **1,** 7 (1991).
2. D. LE BIHAN, E. BRETON, AND A. SYROTA, *C.R. Acad. Sci. (Paris)* **301,** 15 (1985).
3. D. LE BIHAN, E. BRETON, D. LALLEMAND, P. GRENIER, E. A. CABANIS, AND M. LAVAL-JEANTET, *Radiology* **161,** 401 (1986).
4. D. G. TAYLOR AND M. C. BUSHELL, *Phys. Med. Biol.* **30,** 345 (1985).
5. E. L. HAHN, *Phys. Rev.* **80,** 580 (1950).
6. H. Y. CARR AND E. M. PURCELL, *Phys. Rev.* **94,** 630 (1954).
7. E. O. STEJSKAL AND J. E. TANNER, *J. Chem. Phys.* **42,** 288 (1965).
8. E. O. STEJSKAL, *J. Chem. Phys.* **43,** 3597 (1965).
9. M. E. MOSELEY, Y. COHEN, J. KUCHARCZYK, J. MINTOROVITCH, H. S. ASGARI, M. F. WENDLAND, J. TSURUDA, D. NORMAN, AND P. WEINSTEIN, *Radiology* **176,** 439 (1990).
10. C. B. AHN, S. V. LEE, O. NALCIOGLU, AND Z. H. CHO, *Med. Phys.* **13**(6), 789 (1986).
11. C. THOMSEN, O. HENRIKSEN, AND P. RING, *Acta Radiol.* **28**(3), 353 (1987).
12. M. NEEMAN, J. P. FREYER, AND L. O. SILLERUD, *Magn. Reson.* **90,** 303 (1990).
13. D. LE BIHAN, E. BRETON, D. LALLEMAND, M. L. AUBIN, J. VIGNAUD, AND M. LAVAL-JEANTET, *Radiology,* **168,** 497 (1988).
14. R. TURNER, AND P. KELLOG, Progress in NMR spectroscopy, in press.
15. H. E. AVRAM, AND L. E. CROOKS, *in* "Book of Abstracts, Society of Magnetic Resonance in Medicine" p. 80, 1988.
16. R. TURNER, D. LE BIHAN, J. MAIER, R. VAVREK, L. K. HEDGES, AND J. PEKAR, *Radiology* **177,** 407 (1990).
17. T. L. CHENEVERT, J. A. BRUNBERG, AND G. P. SHIELKE, *in* "Book of Abstracts, Society of Magnetic Resonance in Medicine" p. 69, 1989.
18. J. F. MAKI, G. P. COFER, AND G. A. JOHNSON, *Radiology* **169**(P), 155 (1988).